Engineering Structures 203 (2020) 109878

Contents lists available at ScienceDirect

Engineering Structures

journal homepage: www.elsevier.com/locate/engstruct

Seismic mitigation performance of structures with viscous dampers under near-fault pulse-type earthquakes

Gaoxing Hu[a,*], Yanan Wang[b], Wei Huang[a], Bin Li[c], Bin Luo[d]

[a] School of Civil Engineering, Xi'an University of Architecture and Technology, Xi'an 710055, China
[b] School of Civil Engineering, Xi'an Technological University, Xi'an 710021, China
[c] School of Urban Planning and Municipal Engineering, Xi'an Polytechnic University, Xi'an 710600, China
[d] Lanzhou University of Technology, Lanzhou 730050, China

ARTICLE INFO

Keywords:
Near-fault pulse-type ground motions
Fluid viscous damper
Pulse period
Seismic response
Energy dissipation distribution

ABSTRACT

This study is aimed at clarifying the seismic mitigation performance of structures with fluid viscous dampers (FVDs) as a function of the characteristics of the near-fault pulse-type (NP) ground motion and the structural dynamic properties. For this purpose, the response spectra and energy response of single-degree-of-freedom (SDOF) structures with FVDs subjected to 20 NP ground motions with different pulse periods T_p are discussed. The seismic response and energy dissipation distribution of multi-degree-of-freedom (MDOF) structures with FVDs are also investigated and compared with those of SDOF structures. The results revealed that although the presence of FVDs produces significant improvements in the seismic response of the structures, the structure may still experience large plastic deformation, which always occurs when T/T_p is less than '1' and T_1/T_p is greater than '1', T and T_1 being pre-earthquake and post-earthquake structural periods. For short period structures (multi-storey) with FVDs, the plastic deformation can be further slightly reduced by making T/T_p and T_1/T_p less than '1' at the same time, so that the structure can be basically kept within the elastic range. However, the intermediate and long period structures (mid-rise and high-rise) with FVDs are more likely to experience large plastic deformation when T/T_p is less than '1', and the floor shear forces may be slightly reduced or even obviously amplified. Furthermore, the current research findings on SDOF structures with FVDs may not be extended directly to MDOF structures with FVDs due to the more complex dynamic properties of MDOF structures.

1. Introduction

The near-fault (NP) ground motions are also called near-source ground motions, which have been widely concerned by seismologists and earthquake engineers because of the serious damage to urban infrastructure caused by recent earthquakes (such as 1971 San Fernando, 1994 Northridge, 1995 Kobe, 2008 Wenchuan, 2016 Kaohsiung). The NP ground motions are close to a ruptured fault, which is strongly influenced by the rupture mechanism, direction of rupture propagation relative to the site and the permanent ground displacement caused by tectonic movement [1]. Forward directivity occurs when the fault rupture propagates toward a site with a rupture velocity close to shear wave velocity [1–4]. The ground motions oriented in this forward directivity path are characterized by abundant long period components, large pulse peak value and short duration. These effects are best observed in the velocity or displacement time history, and the fault-normal component is more severe than the fault-parallel component [5,6]. When a site is located at one end of the fault and the rupture propagates away from the site, the opposite effect (i.e. backward directivity) can be observed, and the ground motions oriented in this backward directivity path show low amplitude and less long period components.

Furthermore, under the action of tectonic stress, the fault suddenly ruptures when the elastic strains on both sides of the fault accumulate continuously and reach the rupture strength of the fault. The accumulated strain energy releases and produces elastic rebound, which triggers the tectonic earthquake, and produces the permanent static displacement of the ground, namely the fling step. Fling step occurs in the direction of fault slip and therefore is not strongly coupled with the forward directivity [7]. It is generally characterized by a monotonic step in the displacement time history and one-sided pulse in velocity time history. Whereas forward directivity is a dynamic phenomenon that produces no permanent ground displacement and hence two-sided velocity pulses [1]. For strike-slip events, the velocity pulses caused by

* Corresponding author.
E-mail address: hugaoxing@live.xauat.edu.cn (G. Hu).

https://doi.org/10.1016/j.engstruct.2019.109878
Received 24 November 2018; Received in revised form 22 July 2019; Accepted 30 October 2019

forward directivity are mainly shown in the fault-normal components, while the velocity pulses caused by fling step are mainly shown in the fault-parallel components. For dip-slip events, forward-directivity and fling step are both polarized in the fault-normal direction, which may be difficult to distinguish [1].

The increasing ground motion records near a fault rupture indicate that the ground shaking may be characterized by a large, long period velocity and displacement pulse, and can cause serious damage to structures, which holds true particularly in the forward directivity effect [6]. When structures are subjected to this pulse-type ground motions, most of the seismic energy arrives within a short time at the beginning of the record, which may generate high demands and force the structures to dissipate this input energy with few large displacement excursions. Consequently, the risk of failure for structures with insufficient ductility is considerably enhanced. To protect buildings against earthquake disasters, many methods have been developed, one of which is the passive energy dissipation control method. Namely installing considerable passive energy dissipation devices [8] such as viscoelastic dampers, metallic yield dampers, friction dampers and fluid viscous dampers (FVDs) into buildings to mitigate the seismic response, so as to protect the main structure [9–11]. Different passive energy dissipation devices adopt different strategies to achieve this purpose. For example, the friction damper and metal yield damper are displacement dependent, which mainly dissipates seismic input energy through structural displacement deformation. The viscoelastic damper increases structural damping and stiffness, which is displacement and velocity dependent, and its damping effect depends on structural displacement and velocity response. The fluid viscous damper is velocity dependent, which mainly depends on the velocity response of structures to dissipate seismic input energy. Among these devices, FVD is more prevalent due to its wide frequency band of vibration attenuation [12], low cost and easy maintenance. However, the effectiveness of FVDs is less tested by many actual NP earthquakes, although the fact that FVDs can provide significant damping effects under ordinary ground motions has been generally accepted. Whether it is still applicable and effective for such NP ground motions remains to be further studied and confirmed.

Numerous research studies have been carried out in the past decades to investigate the effect of FVD on the seismic mitigation performance of structures subjected to NP ground motions. Tzimas et al. [13] evaluated the collapse risk and residual drift performance of post-tensioned self-centering steel buildings equipped with FVDs, and found that a significant reduction in collapse risk and residual story drift of the structure can be achieved. Zhang and Xi [14] proposed a dimensional analysis method to evaluate the seismic performance of a nonlinear SDOF structure with nonlinear FVDs under NP ground motions, and they found that there exists a critical structure-to-pulse frequency to balance the reduction of structural drift and the increase of the total acceleration. Dicleli and Mehta [15] compared the seismic performance of steel chevron braced frames with and without FVDs, and the result showed that FVDs can improve the structural seismic performance significantly. Tirca et al. [16] discussed the effect of NP ground motions on a middle-rise frame equipped with shear link dampers, which concluded that the structure can be kept in the elastic range. Hatzigeorgiou and Pnevmatikos [17] examined the influence of structural vibration periods, post-elastic stiffness and equivalent viscous damping ratio on the maximum velocity and damping force of SDOF structures with linear FVDs under NP ground motions excitation. Xu et al. [18] compared the different structural damping effects on SDOF structures with FVDs subjected to NP ground motions with varying T/T_p (structural period to pulse period). He and Agrawal [19] proposed an hybrid control system consisting of FVD and a semi-active friction damper, and the result showed that the system is effective in reducing the structural responses.

Most of these studies mainly focus on the seismic response of structures with FVDs, and many conclusions are based on the simplified SDOF structure with FVDs. However, how the total seismic input energy is distributed in the structure is less concerned, which can be used as an important approach to reveal the seismic mitigation performance of structures with FVDs more comprehensively. Thus this study examines the structural seismic mitigation performance in terms of both seismic response and energy dissipation distribution. Furthermore, the seismic behaviour between SDOF and MDOF structures with FVDs is also compared in order to determine whether findings on the seismic response characteristics of SDOF structures with FVDs under NP ground motions can be extended to MDOF structures as well. The purpose of this paper is expected to contribute to a further understanding of the structural seismic behaviour and the action mechanism of NP ground motions. The current research may have important implications on the seismic design and retrofitting of structures located in near-fault seismic regions using FVDs.

2. Selection of NP ground motion records

According to the definition of near-fault seismic region proposed by Ming [20], a number of near-fault ground motion records were download from the database of the Pacific Earthquake Engineering Research (PEER) Center. These records are restricted to strike-slip fault mechanism with moment magnitude M_W greater than 5. The equivalent shear wave velocity of soil Vs30 (Vs30 is the average shear wave velocity in the upper 30 m) is between 250 m/s and 500 m/s, which corresponds approximately to the site class II specified in Chinese code [21]. The pulse indicator I_p proposed by Baker [22] was employed to determine whether the selected records are pulselike. I_p, shown in Eq. (1), takes values between 0 and 1, with high values providing a strong indication that the ground motion is pulselike. The record is considered as pulse when it meets all three of the potential criteria: (1) I_p is greater than 0.85; (2) the peak ground velocity (PGV) of the ground motion is greater than 30 cm/s; (3) the time $t_{20\%,orig}$ at the 20% of the total cumulative squared velocity for the original ground motion is greater than the time $t_{10\%,pulse}$ at the 10% of the total cumulative squared velocity for the extracted pulse.

$$I_p = \frac{1}{1 + e^{-23.3+14.6(PGV\ ratio)+20.5(energy\ ratio)}} \tag{1}$$

Finally, 20 NP ground motion records with forward directivity were picked out and separated into four groups (G1–G4) according to their velocity pulse period T_p, which have been used to investigate the seismic behaviour of SDOF and MDOF structures with FVDs. The records are classified as G1 group when $0.50\,s \le T_p \le 1.10\,s$, G2 when $1.30\,s \le T_p \le 2.40\,s$, G3 when $3.70\,s \le T_p \le 4.70\,s$, G4 when $7.10\,s \le T_p \le 9.50\,s$. Table 1 lists the basic characteristics of the recorded motions. T_p is the velocity pulse period, and PGA is the peak ground acceleration of the ground motions.

3. Influence of various factors on structural seismic mitigation performance

3.1. Dynamic equilibrium equation of SDOF structure

For the sake of simplicity, an idealized one-storey structure with FVDs is first considered, as shown in Fig. 1. It is assumed that a mass is concentrated at the roof level, and a massless frame provides the lateral stiffness of the structure. The axial deformation of the columns is not considered. The Maxwell model is employed to describe the mechanical behaviour of FVD. When the structure remains in the elastic range during the earthquake, the dynamic equation of a SDOF structure with FVDs subjected to ground acceleration $\ddot{x}_g$ can be described by the set of Eqs. (2), where m, c and k are the structural mass, inherent damping coefficient and lateral stiffness. x, $\dot{x}$ and $\ddot{x}$ represent the displacement, velocity and acceleration of the structure relative to the ground, respectively. c_d and α_0 are the damping coefficient and the velocity

Table 1
NP ground motion records in site classII.

Group	No.	Earthquake	Component	Magnitude (M_W)	Fault distance (km)	Vs30 (m/s)	PGA (g)	PGV (cm/s)	I_P	T_p(s)
G1	n4126	Parkfield	360	6.00	3.79	260.63	0.83	39.77	0.99	0.57
	n4126	Parkfield	090	6.00	3.79	260.63	0.68	35.97	1.00	0.64
	n568	San	180	5.80	6.30	489.34	0.70	79.88	0.98	0.85
	n1602	Duzce	090	7.14	12.04	293.57	0.81	65.85	1.00	0.88
	n569	San	270	5.80	6.99	455.93	0.53	72.95	1.00	1.02
G2	n4115	Parkfield	360	6.00	2.65	265.21	0.31	46.87	1.00	1.38
	n1119	Kobe	090	6.90	0.27	312.00	0.61	86.21	1.00	1.89
	n1120	Kobe	000	6.90	1.47	256.00	0.62	120.61	0.95	1.86
	n6906	Darfield	35 W	7.00	1.22	344.02	0.71	100.28	0.99	2.24
	n569	San	180	5.80	6.99	455.93	0.40	56.35	0.98	2.33
G3	n171	Imperial Valley	270	6.53	0.07	264.57	0.30	92.57	1.00	3.56
	n316	Westmorland	315	5.9	16.66	348.69	0.15	32.69	0.92	3.75
	n6911	Darfield	72E	7.00	7.29	326.01	0.48	69.82	0.97	4.02
	n1176	Kocaeli	150	7.51	4.83	297.00	0.32	71.85	0.97	4.54
	n6962	Darfield	61 W	7.00	1.54	295.74	0.32	56.97	0.98	4.64
G4	n6962	Darfield	29E	7.00	1.54	295.74	0.39	85.69	1.00	7.14
	n900	Landers	270	7.28	23.62	353.63	0.25	51.10	1.00	7.50
	n6897	Darfield	27 W	7.00	8.46	295.74	0.26	39.39	1.00	7.66
	n6897	Darfield	63E	7.00	8.46	295.74	0.24	67.22	1.00	7.93
	n6960	Darfield	04 W	7.00	13.64	293.00	0.23	62.69	0.99	9.35

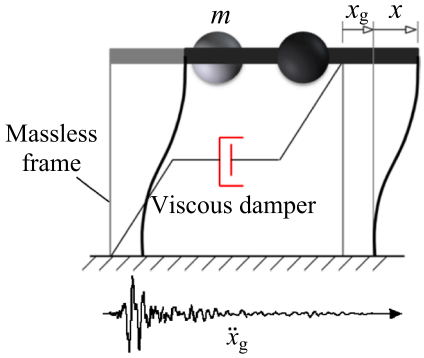

Fig. 1. An idealized shear model of SDOF structure with FVDs subjected to earthquake; x_g and $\ddot{x}_g$ are the ground displacement and acceleration, respectively.

exponent of FVD. In Eq. (2b), the exponent α_0 of FVD controls the damper nonlinearity and its typical value is in the range of 0.35–1 for seismic applications [16,18,24]; F is the damping force of FVD.

$$m\ddot{x} + c\dot{x} + kx + F = -m\ddot{x}_g \tag{2.a}$$

$$F = c_d\ |\dot{x}|^{\alpha_0}\mathrm{sgn}(\dot{x}) \tag{2.b}$$

Assuming that the damper coefficient c_d is proportional to the damping c of the structure, a dimensionless parameter β can be defined as $\beta = c_d/c$; hence, the Eqs. (2) can be rewritten as,

$$\ddot{x} + 2\omega\xi(\dot{x} + \beta\ |\dot{x}|^{\alpha_0}\mathrm{sgn}(\dot{x})) + \omega^2 x = -\ddot{x}_g \tag{3}$$

It has to be recognized that, in strong earthquakes, most structures employing FVDs will experience some level of inelastic response, which may cause significant increases in the base shear [23]. Therefore, the influence of structural nonlinearity on the seismic response has been considered in this paper. The bilinear force-deformation relationship is used to represent the behavior of the SDOF structure when the structure is in the elastoplastic range, as shown in Fig. 2, but degradation of stiffness or strength, or pinching of the hysteresis loop is not considered. Then, a new equation is written in Eqs. (4). In the Eqs. (4), $f(x)$ is the restoring force, α_1 is the post-yield stiffness ratio and x_y is the yielding displacement. When F is 0, the Eqs. (4) can be used to present the elastoplastic SDOF structure without FVDs.

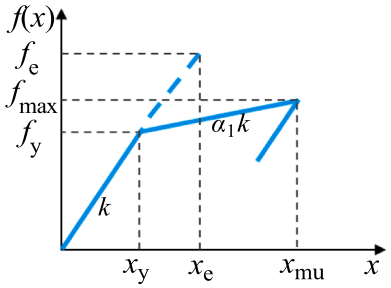

Fig. 2. Bilinear force-deformation relationship of a SDOF structure.

$$m\ddot{x} + c\dot{x} + f(x) + F = -m\ddot{x}_g \tag{4a}$$

$$f(x) = \begin{cases} kx, & x \leqslant x_y \\ \alpha_1 kx + (1-\alpha_1)kx_y, & x_y < x \end{cases} \tag{4b}$$

The maximum force response of an elastic structure can be denoted by f_e, and the yield strength of a nonlinear structure can be denoted by f_y. Then, the force reduction factor R can be defined as $R=f_e/f_y=mS_a/f_y$, where S_a is the maximum acceleration response of the corresponding elastic structure, and the yield strength f_y can be expressed in terms of the yield displacement x_y and elastic stiffness k as $f_y = k \bullet x_y$. The ductility factor μ is defined as the ratio of the maximum inelastic to yield displacement, i.e., $\mu = x_{mu}/x_y$, where x_{mu} is the structural maximum inelastic displacement. Thus, the Eqs. (4) can be rewritten as,

$$\ddot{\mu} + 2\xi\omega(\dot{\mu} + \frac{\beta\omega^2 R}{S_a}\left|\dot{\mu}\frac{S_a}{\omega^2 R}\right|^{\alpha_0}\mathrm{sgn}(\dot{\mu})) + \omega^2\frac{f(x)}{f_y} = -\frac{\omega^2 R}{S_a}\ddot{x}_g \tag{5}$$

3.2. Energy balance equation of SDOF structure

The cumulative energy dissipation of the structure in Eqs. (4) can be obtained by integrating Eqs. (4) with a displacement increment dx as,

$$\int_0^t m\ddot{x}dx + \int_0^t c\dot{x}dx + \int_0^t f(x)dx + \int_0^t Fdx = -\int_0^t m\ddot{x}_g dx \tag{6}$$

where each integral expression represents the cumulative energy from 0 to t time. On the left side of Eq. (6), the first, second, third and fourth terms represent kinetic energy E_K, inherent damping energy E_D, strain energy which contains elastic strain energy E_S and plastic strain energy

E_H, and energy dissipated by FVD, respectively, i.e.,

$$E_K = \int_0^t m\ddot{x}dx,\quad E_D = \int_0^t c\dot{x}dx$$

$$E_S + E_H = \int_0^t f(x)dx$$

$$E_V = \int_0^t Fdx = \int_0^t c_d\ |\dot{x}_d|^{\alpha_0}\ \mathrm{sgn}(\dot{x}_d)dx \tag{7}$$

The total seismic input energy in the structure, E_{inp}, can be obtained by integrating the right side of Eq. (6),

$$E_{inp} = -\int_0^t m\ddot{x}_g dx \tag{8}$$

Finally, the Runge-Kutta numerical differential algorithm [25] was used to solve the Eqs. (3), (5) and (6), respectively. The results of structural seismic response and energy dissipation distribution under NP ground motions excitation can be obtained.

3.3. Discussions on the influence of various factors

To demonstrate the influence of structural dynamic properties on the seismic mitigation performance, SDOF structures with and without FVDs subjected to the Kobe earthquake (n1120) were used to discuss the seismic behaviour, as shown in Fig. 3.

This structure has the inherent damping ratio 2%, and structural foundational period is assumed to be 0.5 s, respectively. Based on the conclusion [15,18] about the effect of damping ratio on seismic response, a typical added effective damping ratio 30% and a velocity exponent 0.4 is considered. The calculated damping ratio of the dampers is solely used as a reference value for the SDOF structures to demonstrate the effect of a level of damping on the seismic response, and the influence of the velocity exponent on the damping ratio is not considered in the analyses of this section. The influence of structural nonlinearity was investigated by assuming that the force reduction factor R [31] equals 3, 5 and 8, and the post-yield stiffness ratio α_1 equals 0.05. A typical NP ground motion (the Kobe earthquake, n1120 in Table 1) is selected as seismic excitation to discuss the influence of structural nonlinear properties on the seismic behavior of SDOF structures.

Fig. 3(a–b) compare the maximum story drift and story acceleration of SDOF structures with and without FVDs, and an index DR is used to quantify the damping effect, which is expressed as DR=($S_{no\_damper} - S_{damper}$)/$S_{no\_damper}$. S_{damper} and S_{no_damper} represent the seismic response (or energy response) of the structure with and without FVDs, respectively. Fig. 3(c) shows the maximum ductility demand corresponding to the structural story drift. It can be found that the variation of the structural nonlinear properties produces great fluctuations in the maximum story drift of SDOF structures without FVDs. At the same time, the acceleration responses decrease obviously when the structure is in the inelastic range. By comparison, the presence of FVDs could significantly reduce the storey drift and acceleration, and keep the seismic responses at a stable level with low dispersion. Furthermore, the ductility demand of the structure can be kept at a low level. Thus, FVDs are observed to be very efficient in mitigating the structural seismic responses, consistent with research by Dicleli [15]. However, it can be observed from Fig. 3(b) that the acceleration response is less reduced or even amplified (when DR is negative) with the increase of the severity of structural nonlinearity. For example, when the structure is in the inelastic range with $R = 8$, the acceleration response of the structure is amplified by 48% due to the presence of dampers, as shown in Fig. 3(b). This indicates that the damping effect of dampers is gradually weakened in terms of acceleration response when the structure is in the inelastic range. Therefore, a balance strategy between the reduction of structural drift and the increase of the total acceleration should be considered when dampers are employed, and this behaviour of SDOF structures with FVDs has been confirmed by Zhang and Xi [14].

Fig. 3(d–e) present the plastic strain energy and the energy dissipated by dampers of the SDOF structure, and Fig. 3(f) compares the energy distribution of the structure with and without FVDs. Columns 1 to 4 in Fig. 3(f) correspond to the elastic structure ($R = 1$) and elasto-plastic structures without FVDs ($R = 3$, $R = 5$, and $R = 8$), respectively, and columns 5 to 8 correspond to those with FVDs. It can be observed that the plastic strain energy increases gradually with the increase of the severity of structural nonlinearity. When the structure is equipped with FVDs, most of seismic input energy can be dissipated by dampers,

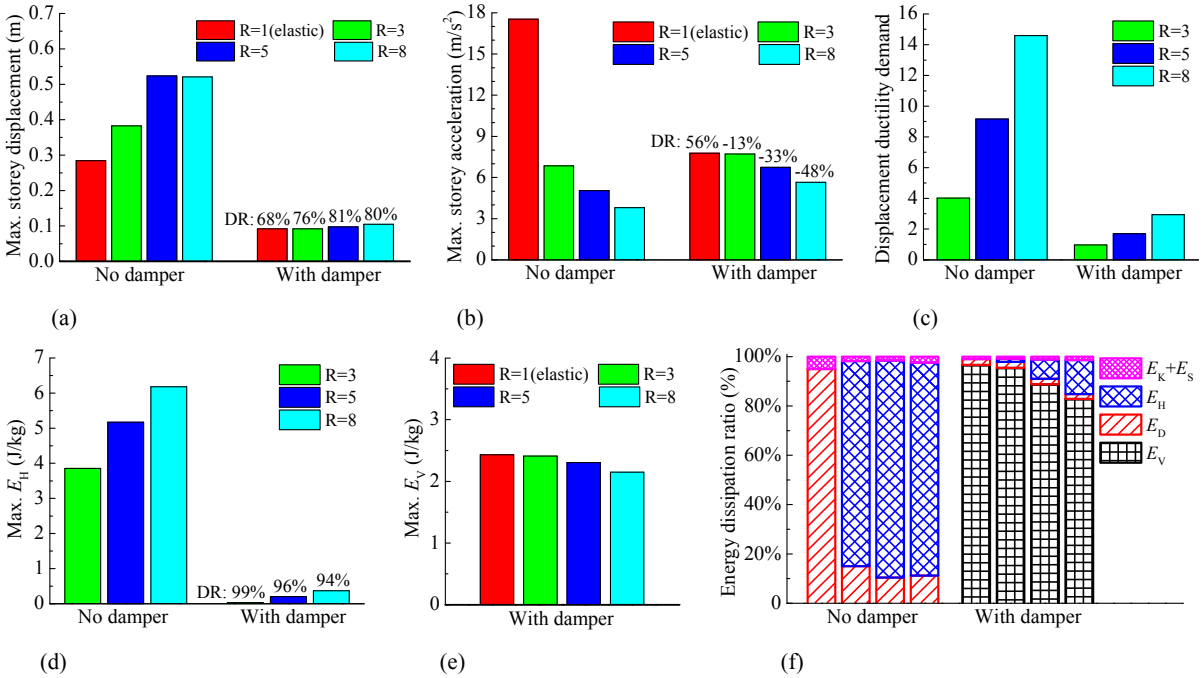

Fig. 3. The maximum seismic response and energy response of SDOF structures with and without FVDs subjected to the Kobe earthquake (n1120): (a) maximum storey drift; (b) maximum storey acceleration; (c) ductility demand; (d) Plastic strain energy; (e) energy dissipation of FVD; (f) energy dissipation ratio.

and the proportion of plastic strain energy to the total seismic input energy is significantly reduced. However, the seismic energy dissipated by dampers decreases obviously when the structure experiences serious inelastic deformation such as $R = 8$. For example, when the force reduction factor R increases from 1 to 8, the energy dissipated by the corresponding damper decreases by 12.75%, as shown in Fig. 3(e). Meanwhile, when the structure experiences some level of inelastic response such as $R = 3$, the energy dissipated by the damper is close to that of the corresponding elastic structure. Thus increasing the lateral yielding strength of structures with FVDs properly such as $R \leq 3$ enables the energy dissipation capacity of FVD to be fully utilized.

3.4. Pulse-type response spectra and energy response

The spectral displacement and acceleration of an elastoplastic SDOF structure ($R = 3$) without and with FVDs (the added effective damping ratio of the damper is 30%, and the velocity exponent is 0.4) are compared to demonstrate the seismic mitigation characteristics of SDOF structures with FVDs under the four groups of NP ground motions. The period of the SDOF system is increased from 0.1 to 6.0 s with an increment of 0.1 s. Since the pulse periods of the G4 group of ground motions are greater than 6.0 s, only the response spectra of the first three groups (G1-G3) are presented in this section. In order to eliminate the influence of different amplitudes (PGA and PGD) of NP ground motions on the response spectra, the spectral displacement *SD* and spectral acceleration *SA* are normalized by the corresponding PGD and PGA, which can be defined as,

$$\beta_{SD} = \frac{SD}{PGD}, \quad \beta_{SA} = \frac{SA}{PGA}$$

Fig. 4(a) compares the average spectral displacement (β_{SD}) when the structures with and without FVDs are subjected to G1-G3 groups of ground motions. The pulse period T_p used in this section is the average value of each group of ground motions. It can be observed from Fig. 4(a) that the displacement response increases obviously with increase in T_p when $T < T_p$ and decreases slowly with increase in T when $T > T_p$, and a large value of displacement usually occurs when T is close to T_p. When the structure is equipped with FVDs, the damping effect of dampers on the displacement response is remarkable when $T/T_p \leq 1$, and it is gradually weakened with increase in T when $T/T_p > 1$. Fig. 4(b) shows plot of the average spectral acceleration (β_{SA}) for the corresponding structures. It can be found that the dynamic amplification effect of the NP ground motions on the inelastic structures without FVDs is significantly weakened with the increase of T. However, the presence of dampers produces obviously amplification in the acceleration response of the SDOF structures. The amplification of acceleration response almost covers the whole period range (0.1–6.0 s) of the response spectra, and does not depend on the pulse period of NP ground motions.

To further clarify the influence of NP ground motions on the behaviour of the structure, the energy response of the corresponding SDOF structure with FVDs subjected to G1–G4 groups of ground motions is presented in Fig. 5. It is noted that the input energy of the structure with FVDs is more than that in the structure without FVDs in some period ranges, which may not be always true. The increased input energy can be mainly explained by the biasing of the power time history in the case of the structure with FVDs that towards one direction [26]. Although the total input energy has been known as a poor index for structural response, it can be observed that the changing trend of the energy dissipated by FVDs relative to the total input energy shows obvious regularity. This characteristic of energy response can be categorized into two categories according to the ratio of T/T_p.

When $T/T_p < 1$, the maximum input energy of the structure with FVDs increases with increase in T, with most of the input energy being dissipated by FVDs. Thus, the FVD is found to be very efficient in reducing the structural seismic response. When $T/T_p > 1$, the energy dissipated by FVDs relative to the maximum input energy of the structure decreases with increase in T, which shows that the damping effect of FVDs on the structure is gradually weakened. Some of the total seismic input energy is converted into kinetic and strain energy that may cause the structure to undergo excessive deformation and amplify the acceleration response.

4. Seismic mitigation performance of MDOF structure

In practical terms, all the buildings are MDOF structures, which is characterized by multiple modes. Thus their dynamic property and seismic response are more complex than those of SDOF structures. In order to reveal the seismic behaviour of structures and the action mechanism of NP ground motions more accurately, MDOF structures have been investigated in terms of the seismic response and energy dissipation distribution.

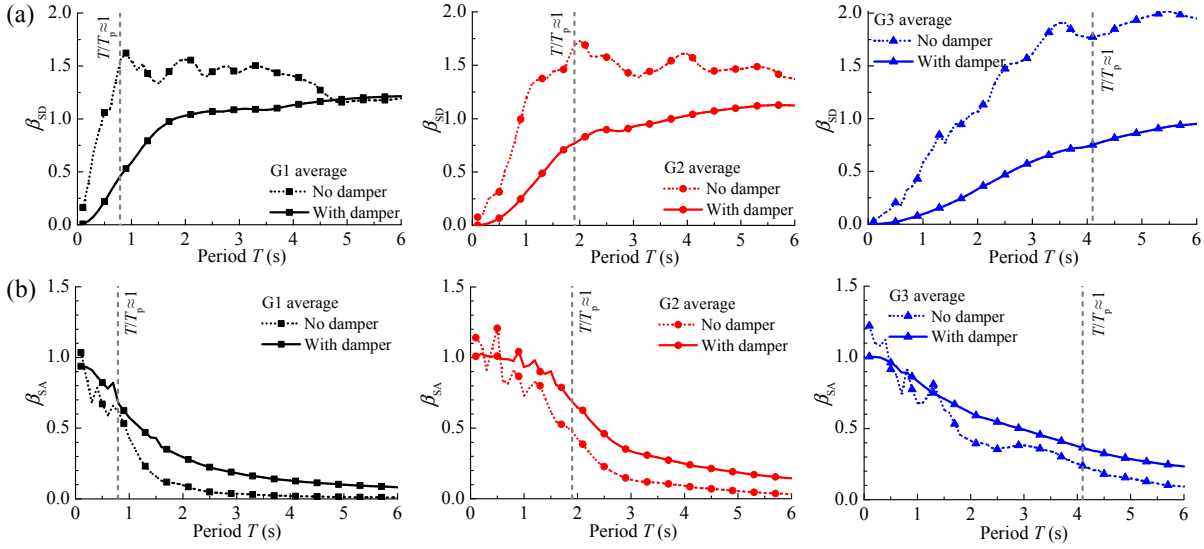

Fig. 4. Average displacement and acceleration spectra; (a) normalized displacement spectra for the structures with and without FVDs; (b) normalized acceleration spectra for the structures with and without FVDs.

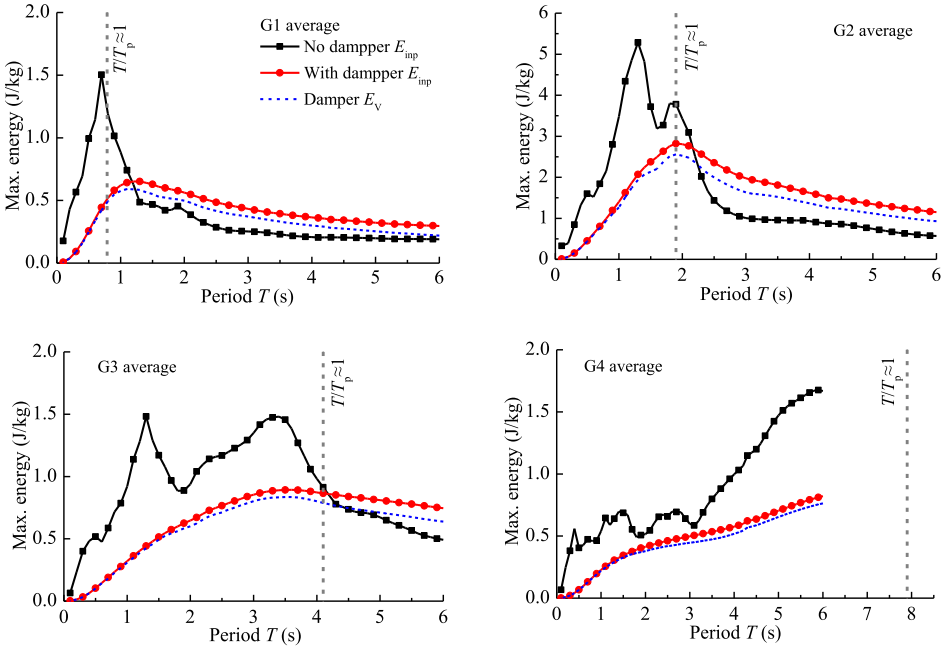

Fig. 5. Average maximum energy response for the SDOF structure.

4.1. Information of the frames considered for analyses

First of all, three generic buildings of four, eight and twelve-storey steel moment-resisting frames are designed in accordance with the Code for Seismic Design of Buildings (GB50011, 2010) [21]. In the Chinese code (GB50011, 2010), a "two-stages-and-three-levels" method is specified for seismic design of building structures. The "three-levels" refers to small, moderate and large intensity earthquakes. Its corresponding structural performance objectives are immediate occupation without damage, normal operation with repairable damage, and collapse prevention. These objectives are achieved by examining forces and elastic displacements under small earthquakes, and by examining the elastoplastic displacements under large earthquakes, which is the so called "two stages" [30]. At the same time, the requirement of some constructional details should be satisfied for the moderate earthquakes. The inherent damping ratio of the structures is 0.02. According to the requirement of the Code for Seismic Design of Buildings (GB50011, 2010), the method of modal decomposition response spectrum is used to check the performance of structures under small earthquakes, and the nonlinear dynamic time history analysis is used to check the elastoplastic displacements under large earthquakes. In order to facilitate the comparison of seismic behavior of the structures under the same seismic intensity, the peak accelerations of the NP ground motions listed in Table 1 are scaled down to 0.5 g to commensurate with the large intensity earthquakes [15].

Thus, three steel moment-resisting frames meeting the requirements of the Chinese code (GB50011, 2010) are obtained. The frames correspond to the multi-storey, mid-rise and high-rise buildings according to the Code for Design of Civil Buildings (GB50352, 2005) [28] (namely the one to three-storey structure is low-storey, the four to six-storey structure is multi-storey, the seven to nine-storey structure is mid-rise and the ten or more than ten-storey structure is high-rise residential building, respectively). They are designed as regular structures, with the base shear coefficients γ [6] being 0.37, 0.20, and 0.13, for the four, eight, and twelve-storey structures, respectively. The base shear coefficients γ is defined as the base shear V that causes yielding in the structure divided by the seismic weight W of the structure. Assuming that the moment-resisting frames without FVDs dissipate energy in the plastic hinges formed in beams, and the base shear V can be expressed in terms of the yield displacement x_y and the elastic stiffness k of the bottom floor of the structures as $V = k \cdot x_y$. The structures consist of three bays (7.2 m, 8.0 m and 7.2 m long) in the weak direction and three bays (6.4 m, 8.0 m and 6.4 m long) in the strong direction. The storey height of each frame is 3.6 m. The dead and live loads of each floors are 3.5 kN/m^2 and 2.0 kN/m^2, respectively. Since the structures are only loaded along the weak axis in this study, details about these structures in the weak direction are listed in Table 2. In this table, the values of the first three periods of vibration of each frame are reported. The fundamental periods of the structures are 0.78 s, 1.60 s and 2.42 s, which can be used to represent short, intermediate, and long period structures, respectively.

To reduce computational efforts, the structures are simplified as idealized MDOF shear models. The models are based on the assumption that floors and ground are rigid, columns are massless, and lumped masses are concentrated at the floor level. A MATLAB program of a structure with FVDs is written for conducting a series of nonlinear time history analysis. The Runge-Kutta numerical differential algorithm is used to iterate within each time step. A bilinear non-degrading hysteresis model is employed to describe the characteristics of the structural nonlinearity. Meanwhile, the yield displacement is determined to

Table 2
Information of steel moment-resisting frames in the weak direction.

Steel frame	Seismic weight W (kg)	Base shear V (kN)	Base shear coefficient γ	Natural vibration period (s)		
				Mode No.1	Mode No.2	Mode No.3
Four-storey	2.48×10^6	0.92×10^4	0.37	0.78	0.29	0.19
Eight-storey	5.05×10^6	1.01×10^4	0.20	1.60	0.56	0.35
Twelve-storey	7.84×10^6	1.02×10^4	0.13	2.42	0.86	0.52

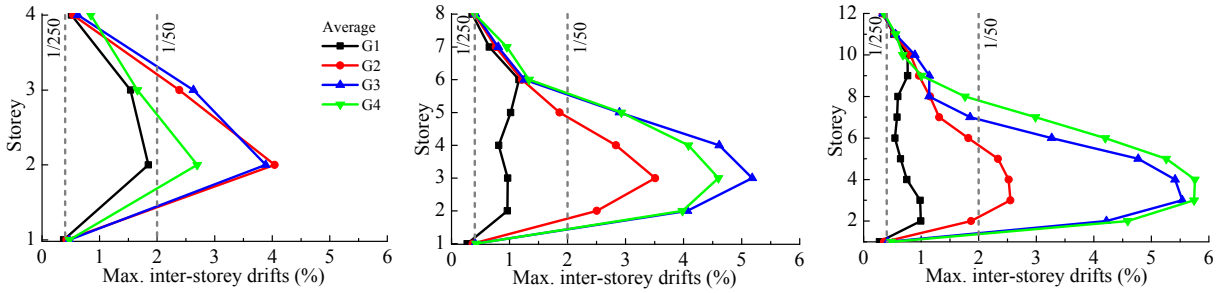

Fig. 6. Maximum average inter-storey drifts of structures without FVDs.

be 1/250 of each storey height according to the Chinese code (GB50011, 2010), and the post-yield stiffness ratio α_1 is assumed to be 0.05.

Then, a reasonable configuration of FVDs in the structure should be considered in order to reflect its damping effect. Losanno [29] pointed out that the uniform FVD distribution may not be the optimal solution in terms of displacement and acceleration responses, and distributing the FVDs along the building is always beneficial to reduce the maximum damper forces. Dicleli [15] recommended that it would be more efficient to place FVDs with relatively larger damping capacity at the lower stories because the relative damper velocities are generally smaller at higher stories, thus producing less damping effect compared to those at lower stories. Fig. 6 shows plots of the maximum average inter-storey drifts of the three structures without FVDs under five groups of NP ground motions. According to the Chinese code (GB50011, 2010), the limit values of elastic and elastoplastic inter-storey drifts are 1/250 and 1/50, respectively. It can be observed that the large deformations usually occur at the intermediate and lower stories of structures, while the upper stories have little deformation. The acceleration responses reflect a similar changing trend, which are not presented in this section. Therefore, a triangular damping distribution along the structural height is considered, which is more reasonable than a uniform placement.

Furthermore, in order to illustrate the seismic mitigation performance of structures with FVDs at a certain level of added effective damping ratio ξ_1, an estimation method for ξ_1 proposed by Banazadeh [27] is presented as,

$$\xi_1 = \frac{T^{2-\alpha_0}\sum_j C_{dj}(\phi_j - \phi_{j-1})^{1+\alpha_0}}{(2\pi)^{3-\alpha_0}\sum_j m_j\phi_j^2}\frac{2^{2+\alpha_0}\Gamma^2(1+\alpha_0/2)}{\Gamma(\alpha_0+2)} \tag{9}$$

where T is the fundamental period of the elastic structure. ϕ_j is the first mode displacement in the horizontal direction at the jth floor level. C_{dj} and m_j are the damping coefficient for FVD and mass of the jth floor level, respectively.

According to the seismic responses of the structures without FVDs, the severity of story deformation can be approximately categorized into three levels: serious elastoplastic deformation, approximately elastic deformation and the level between them. In order to simplify the damper placement, it is assumed that stories in the same level of deformation have same dampers. The FVDs have been classified into three groups (C_{d1}, C_{d2}, C_{d3}, assuming $C_{d2} \approx 0.75C_{d1}$, $C_{d3} \approx 0.5C_{d1}$, and the velocity exponent is 0.4 for C_{d1}, and 0.6 for C_{d2} and C_{d3}) corresponding to the three levels of deformation along the structural height. Based on the relative severity of the three levels of deformation, the coefficient 0.75 and 0.5 are approximately estimated. Then, the damping coefficients of dampers at each floor have been determined according to the Eq. (9) when the added effective damping ratio ξ_1=10%. A reasonable configuration of FVDs in the structures has been shown in Table 3.

Finally, the nonlinear dynamic time history analysis of four, eight and twelve-storey structures with FVDs subjected to NP ground motions is conducted, and the results of comparison between the seismic responses of the structures with and without FVDs are presented in Fig. 7 and Fig. 8.

Table 3
Configuration and parameters of FVDs.

Structure		Four-storey	Eight-storey	Twelve-storey
C_{d1} group	Floor	1–2	1–4	1–6
	c_d(kN·s/m)	10,900	8100	6930
	α_0	0.4	0.4	0.4
C_{d2} group	Floor	3	5–6	7–9
	c_d(kN·s/m)	8170	6050	5200
	α_0	0.6	0.6	0.6
C_{d3} group	Floor	4	7–8	10–12
	c_d(kN·s/m)	5450	4050	3460
	α_0	0.6	0.6	0.6

4.2. Results and discussions

Fig. 7(a) and (b) show the average ductility demands of the structures with and without FVDs respectively. x_{mj} and x_{yj} are the maximum displacement response and yield displacement at the jth floor level. μ_y and μ_m are the ductility demands which corresponds to the limit values of 1/250 and 1/50, respectively. Fig. 8(a) presents the floor acceleration ratio R_A, i.e., the ratio of the maximum acceleration (S_{a1}) of structures with FVDs to the maximum acceleration (S_{a0}) of structures without FVDs. Fig. 8(b) presents the floor shear ratio R_V, i.e., the ratio of the maximum shear force (S_{v1}) of structures with FVDs to the maximum shear force (S_{v0}) of structures without FVDs.

Some obvious characteristics of the structures with different values of γ can be observed from Fig. 7 and Fig. 8, which can be summarized as follows:

(1) As for the short period structure without FVDs such as the four-storey structure, the maximum average ductility demand of the structure subjected to the four groups of NP ground motions varies from 4.62 to 10.10, as shown in Fig. 7(a). When FVDs are installed into the structure, the maximum ductility demand is reduced to 2.42, and the floor shear forces can also be significantly reduced, as shown in Fig. 7(b) and Fig. 8(b). However, it can be observed that parts of the acceleration responses of the structure with FVDs are obviously amplified, as shown in Fig. 8(a), which is similar to that of the SDOF structures with FVDs in the short period range.
(2) With the decrease of base shear coefficient (γ decreases from 0.37 to 0.13), the maximum average ductility demand of the structure without FVDs such as the twelve-storey structure increases to 14.50, and many of the ductility demands exceed the maximum limit μ_m=5, as shown in Fig. 7(a). Besides, it can be observed that the ductility demand of structures subjected to NP ground motions with different pulse periods T_p shows great differences. For example, when the twelve-storey structure without FVDs is subjected to the four groups of NP ground motions, the structural maximum ductility demand varies from 2.50 to 14.50. When the structure is

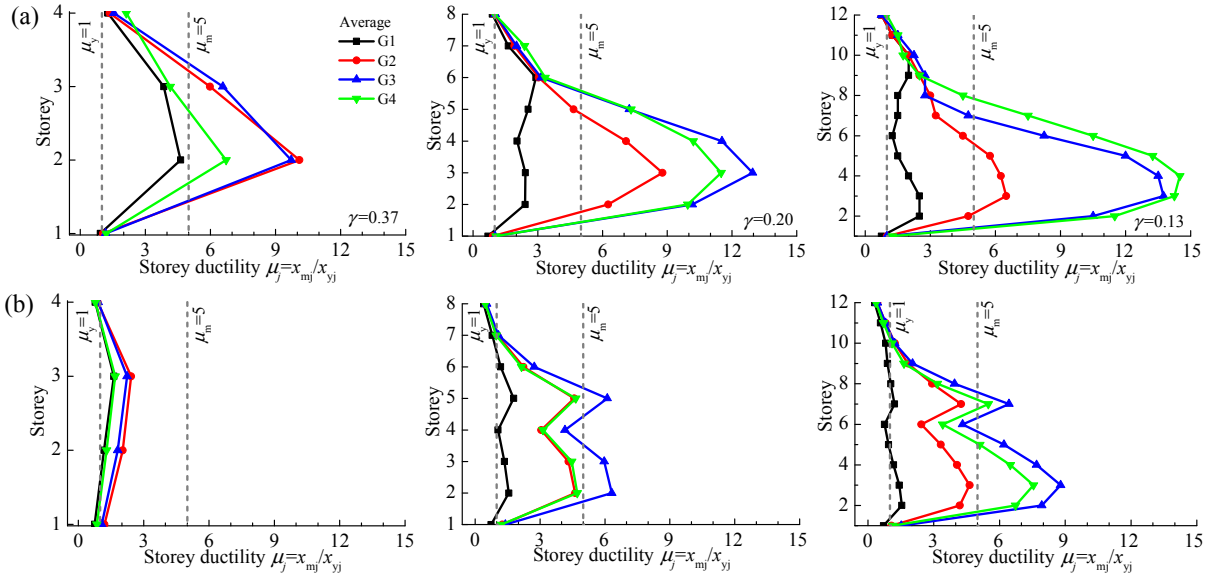

Fig. 7. Seismic responses of the structures: (a) average ductility demands of the structures without FVDs; (b) average ductility demands of the structures with FVDs.

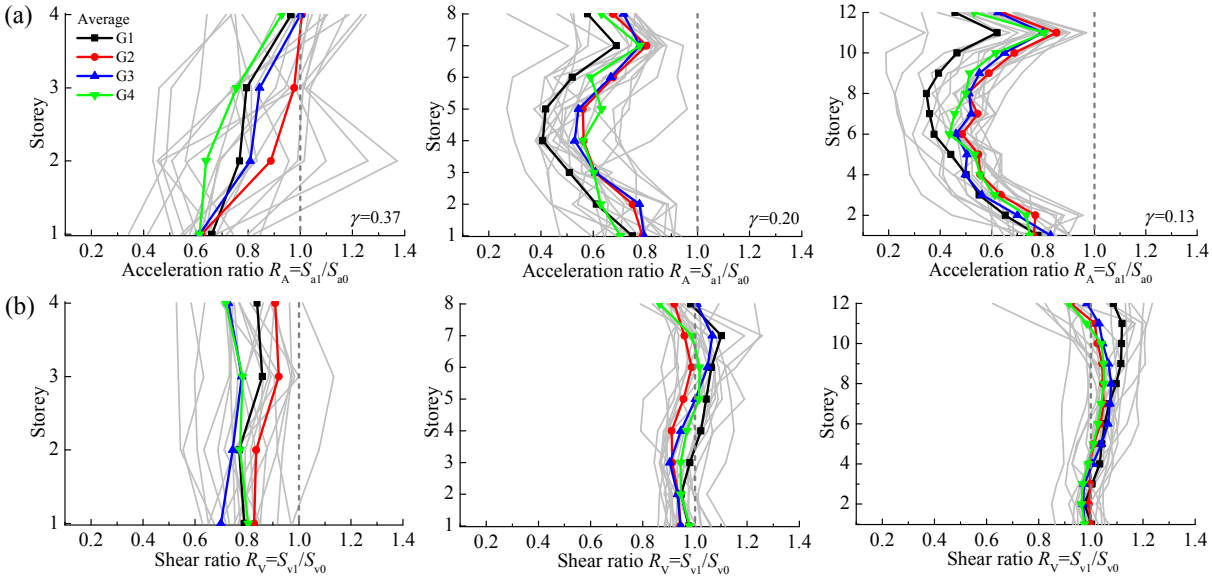

Fig. 8. Seismic responses of the structures with FVDs: (a) floor acceleration ratio; (b) floor shear ratio.

equipped with dampers, the maximum ductility demand decreases significantly, but it still varies from 1.54 to 8.79. This indicates that the pulse period of NP ground motions may play an important role in determining the seismic responses of structures. To further demonstrate the action mechanism of NP ground motions, the influence of the relation between T and T_p on the seismic behaviour of the structures with FVDs is discussed in the Section 4.3.

(3) It can be observed from Fig. 8(a) and (b) that with the increase of the height of structures, the base shear coefficient decreases and the structural fundamental periods are gradually increasing. Compared to structures without FVDs, the acceleration response of structures with FVDs can be gradually controlled, which is quite different from the behaviour of SDOF structures with FVDs in Fig. 4(b). However, the floor shear ratio is increasing, and most of them have exceeded '1' with the decrease of base shear coefficient. This indicates that the floor shear forces may be reduced slightly or even amplified obviously for intermediate and long period structures with FVDs, which will lead to an increase in demand for structural shear strength.

4.3. Energy dissipation distribution

This section studies the influence of the relationship between T and T_p on the seismic behaviour of the structures with FVDs subjected to NP ground motions. The proportion of energy distribution in structures with FVDs and the corresponding period ratios of the structures are presented in Fig. 9.

Fig. 9(a)-(c) show plots of the energy distribution of the four-storey, eight-storey and twelve-storey structures with FVDs. It can be observed that the changing trend of the proportion of plastic strain energy E_H under the four groups of ground motions is basically consistent with the variation of structural ductility demands in Fig. 7(b). Therefore, the proportion of structural plastic strain energy is used to represent the level of plastic deformation and ductility demand, which could facilitate the understanding of the seismic behaviour of the structures. Fig. 9(d–f) present the period ratios (T/T_p and T_1/T_p) of the corresponding structures, where T and T_1 are the pre-earthquake and post-earthquake fundamental periods of structures, respectively. It can be observed that there is a strong correlation between the maximum

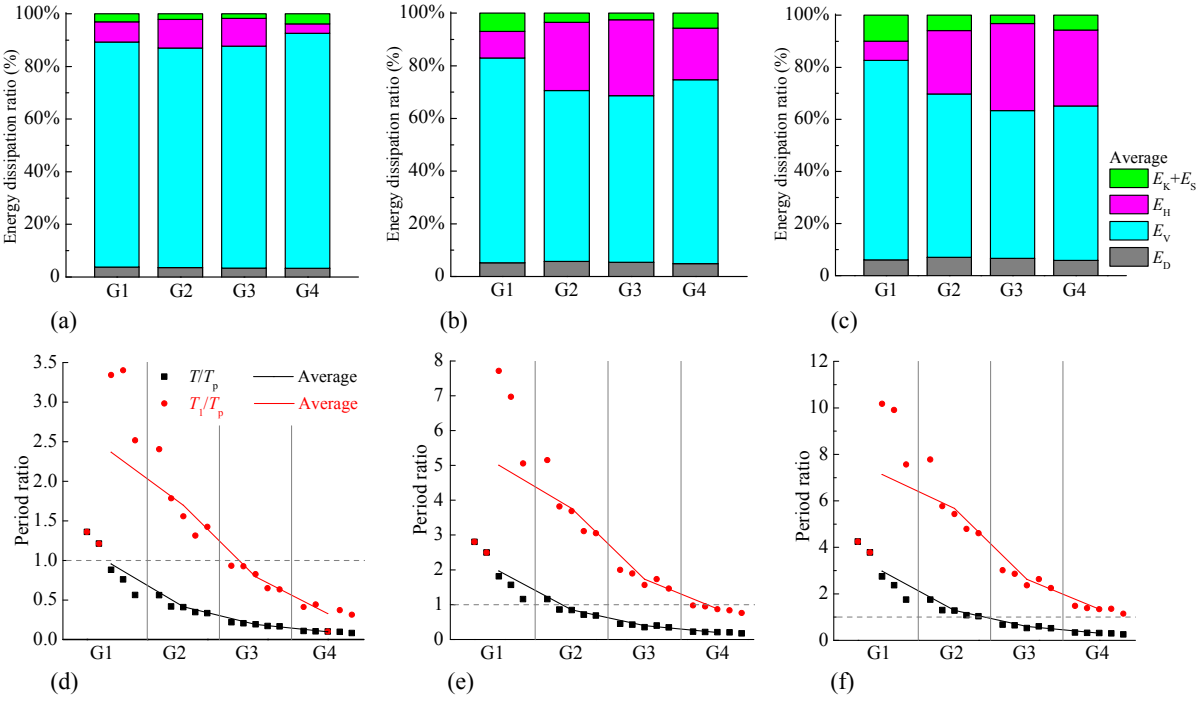

Fig. 9. The average energy dissipation distribution and period ratio of the structures with FVDs: (a), (d) four-storey structure (γ = 0.37); (b), (e) eight-storey structure (γ = 0.20); (c), (f) twelve-storey structure (γ = 0.13).

plastic strain energy and the period ratio.

For a relatively strong short period structure with FVDs such as the four-storey structure with γ = 0.37, as shown in Fig. 9(a), it can be observed that most of the seismic input energy can be dissipated by dampers, and the proportion of plastic strain energy to the total input energy is small. Therefore, the plastic deformation of the structure can be significantly reduced. Furthermore, the plastic strain energy does not change significantly with the variation of period ratio, which indicates that this type of strong short period structure with FVDs is less affected by the NP ground motions with different pulse periods. With the decrease of γ, the structures are becoming flexible, and the large plastic deformation always appears in the structures when $T/T_p < 1$ and $T_1/T_p > 1$. For instance, the large plastic strain energy occurs in the eight-storey structure when subjected to G3 group of ground motions, as well as in the twelve-storey structure subjected to G3 and G4 groups of ground motions, as shown in Fig. 9(b–c). Its corresponding period ratio T/T_p varies from 0.3 to 0.7 and T_1/T_p varies from 1.4 to 3.0, as shown in Fig. 9(e–f). This is because the main vibration periods of the structure are increasing with each floor of the structure yields gradually, and the resonance effect occurs when the main vibration periods approach T_p.

In addition, it can be found that a small plastic strain energy of the structures usually occurs when the structures are in some specific period ranges. For example, when the four-storey structures with FVDs is subjected to G4 group of ground motions, the corresponding T/T_p is less than 0.15 and T_1/T_p is less than 0.50, and only a small plastic strain energy is observed in the structure. At the same time, when T/T_p is greater than 1.5, the minimum plastic strain energy also occurs in the eight and twelve-storey structures with FVDs when subjected to G1 groups of ground motions. The corresponding plastic deformations of the structures in Fig. 7(b) confirmed this seismic behaviour, which indicates that the seismic performance of structures with FVDs can be significantly improved by making the period ratio (T/T_p and T_1/T_p) of structures in a specific range.

From the results of the three buildings discussed above, it is clear that the large plastic deformation always occurs when T/T_p is less than '1' and T_1/T_p is greater than '1'. For a relatively strong structure (multi-storey) with FVDs, its fundamental period is relatively short, and the influence of NP ground motions with different pulse periods on the structural plastic deformation is limited. Nevertheless, the plastic deformation can be further reduced slightly by making T/T_p and T_1/T_p less than '1' at the same time, so that the structure can be basically kept within the elastic range. The intermediate and long period structures (mid-rise and high-rise) with FVDs are relatively flexible, which is more likely to experience the large plastic deformation when T/T_p is less than '1'. Keeping T/T_p greater than '1' is an effective way to reduce the structural plastic deformation.

Based on the above analysis, it can be concluded that the seismic behaviour of the relatively strong structures (multi-storey) with FVDs under NP ground motions is similar to that of the SDOF structures with FVDs. However, for the intermediate and long period structures (mid-rise and high-rise) with FVDs, the seismic behaviour of this kind of MDOF structures perform differently. It strongly depends on the structural dynamic property and input ground motion, which is difficult to be adequately reflected by the SDOF structure model. Therefore, the current research findings on SDOF structures with FVDs subjected to NP ground motions may not be extended directly to MDOF structures with FVDs.

Furthermore, in order to analyze the distribution characteristics of the plastic energy dissipation, Fig. 10 and Fig. 11 show plots of the distribution of plastic strain energy along the height of the four and twelve-storey structures with and without FVDs, respectively. The E_H and E_{Hj} represent the structural total plastic strain energy and the plastic strain energy of the jth floor level.

For structures without FVDs, it can be observed from Fig. 10(a) and Fig. 11(a) that the maximum plastic strain energy is mainly concentrated in the intermediate and lower stories of structures. At the same time, the relatively large plastic strain energy also occurs at the upper stories when the twelve-storey structure without FVDs subjected to G1 group of ground motions, which is mainly due to the significant contributions of higher modes effects. After installing FVDs into the structures, the total plastic strain energy can be significantly reduced, and the relatively maximum plastic strain energy shifts to the floors where the energy dissipation capacity of FVD varies greatly. For example, the relatively large plastic strain energy at the second floor shifts

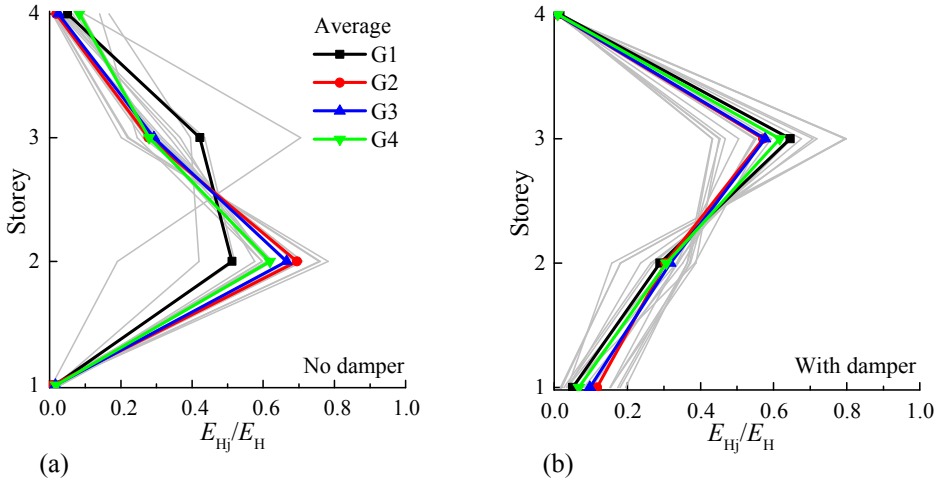

Fig. 10. Energy dissipation distribution of the four-storey structure: (a) the structure without FVDs; (b) the structure with FVDs.

to the third in the four-storey structure, as shown in Fig. 10(a) and (b). Moreover, the large plastic strain energy at the 3rd to 5th floor level shifts to the 7th in the twelve-storey structure, as shown in Fig. 11(a) and (b). Obviously, it can be found that the 3rd floor level in the four-storey structure with FVDs and the 7th floor level in the twelve-storey structure with FVDs are the places where the energy dissipation capacity of FVDs begins to change greatly, as shown in Table 3. Therefore, it can be concluded that the damper has a significantly effect on the plastic distribution of structures, a large plastic deformation of structures may be concentrated at the location where the energy dissipation capacity of dampers in adjacent floors varies greatly. This adverse effect should be considered when using dampers for the seismic design and retrofitting of structures located in near-fault seismic regions.

5. Conclusions

In this paper, the seismic mitigation performance of structures with FVDs under NP ground motion records with forward directivity has been investigated by analyzing seismic response and energy dissipation distribution, and the seismic mitigation performance of SDOF structures and MDOF structures have been compared. The purpose of this paper is expected to contribute to a further understanding of the structural seismic behaviour and the action mechanism of NP ground motions. Meanwhile, it has to be noted that the conclusions in this paper are based on the idealized shear model of steel frames, and the main conclusions of this research are:

(1) For structures with FVDs subjected to NP ground motions, increasing the lateral yielding strength of structures properly are effective in reducing the seismic response. Also, in this way the energy dissipation capacity of dampers can be fully utilized.
(2) Different MDOF structures with FVDs show different seismic behaviour under the influence of T/T_p. For a short period structure (multi-storey) with FVDs subjected to NP ground motions, the severity of plastic deformation and the floor shear forces can be obviously reduced when the structure has a certain level of added effective damping ratio. However, the acceleration responses may be amplified when T/T_p is less than '1' and T_1/T_p is greater than '1'. In this case, the seismic behaviour is similar to that of SDOF structures with FVDs. For longer period structures (mid-rise and high-rise) with the same level of added effective damping ratio, the acceleration responses can be gradually controlled, but the floor shear forces will be slightly reduced or even obviously amplified. The seismic behaviour of this kind of MDOF structures under NP ground motions performs differently, which strongly depends on the structural dynamic property and input ground motion, and it is difficult to be adequately reflected by the SDOF structure model. Therefore, the current research findings on SDOF structures with FVDs subjected to NP ground motions may not be extended directly to MDOF structures with FVDs.

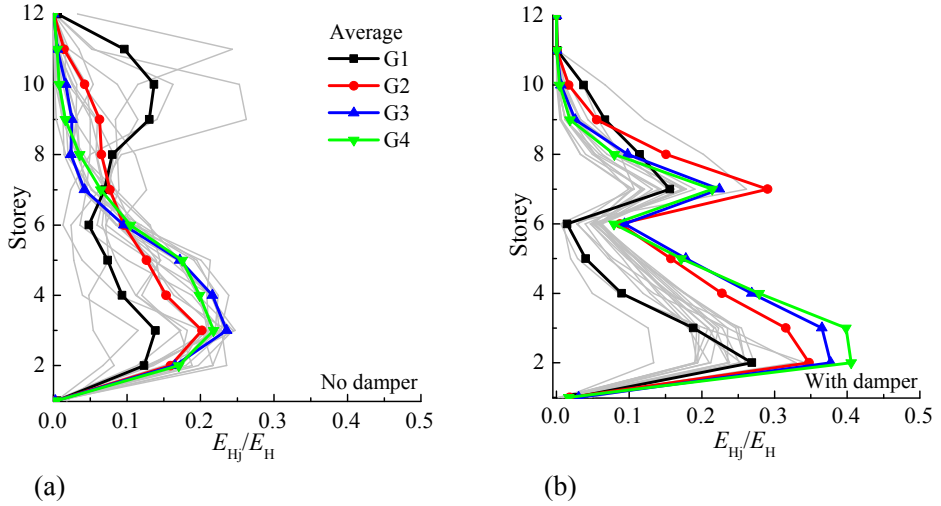

Fig. 11. Energy dissipation distribution of the twelve-storey structure: (a) the structure without FVDs; (b) the structure with FVDs.

(3) The large plastic deformation of structures with FVDs will always occur when T/T_p is less than '1' and T_1/T_p is greater than '1'. For short period structures (multi-storey) with FVDs, the plastic deformation is less affected by the NP ground motions with different pulse periods. Nevertheless, the plastic deformation can be further slightly reduced by making T/T_p and T_1/T_p less than '1' at the same time, so that the structure can be basically kept within the elastic range. However, the intermediate and long period structures (mid-rise and high-rise) with FVDs are more likely to experience the large plastic deformation when T/T_p is less than '1'. Keeping T/T_p greater than '1' is an effective way to reduce the plastic deformation and improve the seismic mitigation performance of the structures.

(4) When structures with FVDs are subjected to NP ground motions, a large plastic deformation may be concentrated at the location where the energy dissipation capacity of dampers in adjacent floors varies greatly. Therefore, this adverse effect should be considered when using dampers for the seismic design and retrofitting of structures located in near-fault seismic regions.

Acknowledgments

The authors are grateful for the financial support impart from the National Natural Science Foundation of China (Grant Nos. 51578446, 51508021 and 51808423) and the Pacific earthquake Engineering Research (PEER) Center. Any opinions, findings, and conclusions or recommendations expressed in this material are those of the authors and do not necessarily reflect those of the National Natural Science Foundation.

References

[1] Bray JD, Rodriguez-Marek A. Characterization of forward-directivity ground motions in the near-fault region. Soil Dyn Earthquake Eng 2004;24(11):815–28.
[2] Mavroeidis GP, Papageorgiou AS. A mathematical representation of near-fault ground motions. Bull Seismol Soc Am 2003;93(3):1099–131.
[3] Somerville PG, Smith NF, Graves RW, et al. Modification of empirical strong ground motion attenuation relations to include the amplitude and duration effects of rupture directivity. Seismol Res Lett 1997;68(1):199–222.
[4] Kalkan E, Kunnath SK. Effects of fling step and forward directivity on seismic response of buildings. Earthquake Spectra 2006;22(2):367–90.
[5] Somerville P. Development of an improved ground motion representation for near fault ground motions. Proceedings of SMIP98 seminar on utilization of strong-motion data, Oakland, CA. 1998.
[6] Alavi B, Krawinkler H. Behaviour of moment-resisting frame structures subjected to near-fault ground motions. Earthquake Eng Struct Dyn 2004;33(6):687–706.
[7] Abrahamson, N., Incorporating effects of near fault tectonic deformation into design ground motions, a presentation sponsored by the Earthquake Engineering Research Institute Visiting Professional Program, hosted by the University at Buffalo; 26 October 2001.
[8] Soong TT, Dargush GF. Passive energy dissipation systems in structural engineering. New York: Wiley; 1997.
[9] Soong TT, Spencer BF. Supplemental energy dissipation: state-of-the-art and state of-the-practice. Eng Struct 2002;24:243–59.
[10] Constantinou MC, Soong TT, Dargush GF. Passive Energy Dissipation Systems for Structural Design and Retrofit. Multidisciplinary Center for Earthquake Engineering Research, State University of New York at Buffalo: New York; 1998.
[11] Foti D. Response of frames seismically protected with passive systems in near-field areas. Int J Struct Eng 2014;5(4):326–45.
[12] Pazooki A, Goodarzi A, Khajepour A, Soltani A, Porlier C. A novel approach for the design and analysis of nonlinear dampers for automotive suspensions. J Vib Control 2017;24:3132–47.
[13] Tzimas AS, Kamaris GS, Karavasilis TL, et al. Collapse risk and residual drift performance of steel buildings using post-tensioned MRFs and viscous dampers in near-fault regions. Bull Earthq Eng 2016;14(6):1643–62.
[14] Zhang Jian, Xi Wang. Optimal nonlinear damping for inelastic structures using dimensional analysis. 20th analysis & computation specialty conference. 2012.
[15] Dicleli M, Mehta A. Effect of near-fault ground motion and damper characteristics on the seismic performance of chevron braced steel frames. Earthquake Eng Struct Dyn 2010;36(7):927–48.
[16] Tirca LD, Foti D, Diaferio M. Response of middle-rise steel frames with and without passive dampers to near-field ground motions. Eng Struct 2003;25(2):169–79.
[17] Hatzigeorgiou GD, Pnevmatikos NG. Maximum damping forces for structures with viscous dampers under near-source earthquakes. Eng Struct 2014;68(8):1–13.
[18] Xu Z, Agrawal AK, He WL, et al. Performance of passive energy dissipation systems during near-field ground motion type pulses. Eng Struct 2007;29(2):224–36.
[19] He WL, Agrawal AK. An innovative hybrid control system for civil structures against near-field earthquakes. Structures congress. 2004.
[20] Li M, Xie L, Zhai C, Yang Y. Scope division of near-fault ground motion. Earthquake Eng Eng Vibrat 2009;29(5):20–5. (in Chinese).
[21] China Ministry of Construction (CMC). Code for seismic design of buildings (GB50011-2010). Beijing, China: China Architecture & Building Press; 2010.
[22] Baker JW. Quantitative Classification of Near-Fault Ground Motions Using Wavelet Analysis. Bull Seismol Soc Am 2007;97(5):1486–501.
[23] Symans MD, Charney FA, Whittaker AS, et al. Energy dissipation systems for seismic applications: current practice and recent developments. J Struct Eng (ASCE) 2008;134(1):3–21.
[24] Lin WH, Chopra AK. Earthquake response of elastic SDOF systems with nonlinear fluid viscous dampers. Earthquake Eng Struct Dyn 2002;31:1623–42.
[25] Ascher UM, Ruuth SJ, Spiteri RJ. Implicit-explicit Runge-Kutta methods for time-dependent partial differential equations. Appl Numer Math 1997;25:151–67.
[26] Seleemah A, Constantinou MC. Investigation of seismic response of buildings with linear and nonlinear fluid viscous dampers. Report No. NCEER 97-0004, National Center for Earthquake Engineering Research, State Univ. of New York at Buffalo, Buffalo, NY; 1997.
[27] Banazadeh M, Ghanbari A. Seismic performance assessment of steel moment-resisting frames equipped with linear and nonlinear fluid viscous dampers with the same damping ratio. J Constr Steel Res 2017;136:215–28.
[28] China Ministry of Construction (CMC). Code for design of civil buildings (GB50352-2005). Beijing, China: China Architecture & Building Press; 2005.
[29] Losanno D, Londono JM, Zinno S, et al. Effective damping and frequencies of viscous damper braced structures considering the supports flexibility. Comput Struct 2017.
[30] Zhou Y, Lu X, Weng D, et al. A practical design method for reinforced concrete structures with viscous dampers. Eng Struct 2012;39:187–98.
[31] Uniform building code. International Conference of Building Officials (ICBO). Whittier,1997; 1234-1253.